OUTSTANDING JUNIOR INVESTIGATOR REPORT FOR L. RANDALL

1992–1997

I. SUPERSYMMETRIC FIELD THEORY AND PHENOMENOLOGY

Much of Lisa Randall's work over the past five years has been aimed at bridging the gap between the exactly supersymmetric world of string theories and the world that we actually observe. Her work on supersymmetry breaking is described in item (1) below, and related work on the mass hierarchy and the relation between supersymmetry and grand unified theories is described in items (2) and (3). Randall's work on distinguishing between supersymmetric models is described in item (4). Randall has also been interested in the fundamental question of how gauge theories arise from D-branes, a topic discussed in item (5).

1. Supersymmetric Field Theory

If we assume that supersymmetry is central to resolving the hierarchy problem (i.e., the puzzle of why $M_{\rm weak} \ll M_{\rm Planck}$), the question of how supersymmetry is broken remains an outstanding problem. In a series of papers, Lisa Randall has explored the question of dynamical supersymmetry breaking, exploiting known results of supersymmetric gauge theories.

The R Axion from Dynamical Supersymmetry Breaking

Randall, Jonathan Bagger (Johns Hopkins), and Erich Poppitz (U. Chicago, now at Johns Hopkins) investigated the mass of the R-axion in generic calculable models of dynamical symmetry breaking [1]. They showed that the axion is massive in any model in which the cosmological constant is fine-tuned to zero through an explicit R-symmetry violating constant. The axion in visible sector models can thereby evade astrophysical bounds, which permitted much simpler models of gauge-mediated supersymmetry breaking.

Low Energy Kähler Potentials in Supersymmetric Theories With (Almost) Flat Directions

Randall and Poppitz investigated the Kähler potentials for the almost flat directions which might exist, for example, in models of dynamical supersymmetry breaking [21]. They derived the supersymmetric low energy effective theory of the D-flat directions of a supersymmetric gauge theory. The Kähler potential of Affleck, Dine, and Seiberg was derived by applying holomorphic constraints which manifestly

DISCLAIMER

DISCLAIMER

Portions of this document may be illegible in electronic image products. Images are produced from the best available original document.

maintain supersymmetry. They also presented a simple procedure for calculating all derivatives of the Kähler potential at points on the flat direction manifold. They illustrated the method on the example of a chiral Abelian model.

Dynamical Supersymmetry Breaking

With graduate students C. Csáki (now at UC Berkeley) and Witold Skiba (now at UC San Diego), Randall [5] studied a model in which a quantum modification of the moduli space does not permit a supersymmetry breaking vacuum. By employing the fact that the superpotential is holomorphic and understanding various limits (as gauge couplings are turned off), she was able to construct the exact superpotential for the model, and also explicitly demonstrated that supersymmetry is broken. A general class of models based on the gauge group $SU(n)\times SU(3)\times U(1)$ was constructed.

Randall, in collaboration with Csáki, Skiba, and Robert Leigh (Rutgers) subsequently studied models based on the gauge groups $SU(n)\times SU(4)\times U(1)$ and $SU(n)\times SU(5)\times U(1)$ [8]. These models were used to demonstrate that theories in the confining, free magnetic, and conformal phases can break supersymmetry through dynamical effects.

The field content of the above theories could be obtained by decomposing an $SU(m)$ theory with an antisymmetric tensor and $m-4$ fundamentals. With Leigh and Riccardo Rattazzi (CERN), Randall investigated the entire class of such models [16]. It was shown that all models of interest could be obtained by the addition of an adjoint superfield and that the dynamics of this model could be obtained from the duality of Kutasov and Schwimmer [R2] and a deconfinement method of Berkooz [R3]. This led to a better understanding of the models described above, and to insights into the relationship between R-symmetry and supersymmetry breaking.

It had been argued that the superpotential can be renormalized in the presence of massless particles, raising the question of whether supersymmetry could be restored by new terms in the superpotential. Randall and Poppitz [22] showed that even in the presence of massless particles, there are no new contributions to the superpotential at any order in perturbation theory.

Further Work on Supersymmetry Breaking

Additional work on supersymmetry breaking included the construction of gauge-mediated supersymmetry breaking models and their implementation through composite dynamics (with Csáki and Skiba) [6, 7]. With two students from Boston University (Bogdan Dobrescu and Indranil Dasgupta) Randall investigated the question of vacuum stability in gauge-mediated models [9].

In future work, Randall intends to continue the search for simple and realistic models of supersymmetry breaking.

2. Supersymmetry and Supergravity

Randall, Jonathan Bagger (Johns Hopkins) and Erich Poppitz (U. Chicago, now at Johns Hopkins), examined the stability of the mass hierarchy in hidden-sector supergravity theories [2]. They showed that a quadratically-divergent tadpole can appear at two loops, even in minimal supergravity theories, provided the theory has a gauge- and global-symmetry singlet with renormalizable couplings to the visible fields. This tadpole can destabilize the hierarchy. They also found a quadratically-divergent two-loop contribution to the field-dependent vacuum energy. This result indicates that one cannot control dangerous divergences and solve for soft parameters in the context of a supergravity theory dynamically.

In the future Randall hopes to study whether there are any circumstances under which one can in fact dynamically determine the low energy soft parameters.

3. Supersymmetric Theories and Phenomenology

There are many signatures for supersymmetric theories which will hopefully be well-studied in the upcoming years. If supersymmetry is discovered, it will be important to be able to discriminate between the underlying models.

With Emanuel Katz and Shufang Su (graduate students), Randall investigated the violation of the equality of the gauge and gaugino couplings in the presence of soft supersymmetry breaking [14, 15]. Although this is a hard supersymmetry breaking effect, finite contributions can be determined as a function of soft supersymmetry breaking masses. The largest sources are "super-oblique" corrections, which can be determined from the two-point function of the gauge boson and gaugino. They showed that the effects can be quite large, particularly in models of supersymmetry breaking motivated by solving the supersymmetric flavor problem.

In current work Randall and Su are investigating how B physics can discriminate between different solutions to the flavor problem of supersymmetric theories. They are focusing on the measurement of an asymmetry in like-sign leptons arising from the decay of neutral B mesons as a way to detect large modifications to the standard model contribution to B meson mixing.

4. Supersymmetry and Grand Unified Theories

An outstanding problem for supersymmetric Grand Unified Theories is to explain why the Higgs triplet is so heavy and the doublet so light. Randall, Zurab Berezhiani (INFN, Ferrara), and Csaba Csáki (graduate student, now at UC Berkeley) investigated whether the supersymmetric Higgs particles can naturally be pseudo-Goldstone bosons [3]. Although it is simple to generate an accidental symmetry of the renormalizable terms of the potential, it is quite difficult to construct a model which allows for the preservation of the accidental symmetry in the nonrenormalizable terms. They

presented three ways to construct a superpotential for which the dangerous mixing terms are sufficiently suppressed, even in the presence of nonrenormalizable interactions. Randall and Csáki subsequently investigated the phenomenology of the Higgs sector of these models [4].

5. D-Branes and Supersymmetric Gauge Theories

Randall has studied the emergence of gauge theories from D-branes. With two MIT graduate students, Joshua Erlich and Asad Naqvi, she determined the low-energy description of $N = 2$ supersymmetric SU(k) product group theories with bifundamental and fundamental matter based on M-theory fivebrane configurations. The dependence on moduli and scales of the coefficients in the non-hyperelliptic Seiberg–Witten curves for these theories is determined by considering various field theory and brane limits.

There is certainly much more to be learned from the interplay of string theory and gauge theory. In particular, the study of chiral theories merits particular attention. Along with graduate student, Emanuel Katz, Randall is continuing to investigate possible candidate brane configurations for such theories. Further advances in gauge theories should be expected based on the many connections being discovered between gauge and string theories.

II. COSMOLOGICAL AND ASTROPHYSICAL APPLICATIONS OF FIELD THEORY

Randall has been most interested in exploring the implications of supersymmetry for cosmology. Item (1) below contains a description of her work (with collaborators) on the cosmological moduli problem, cosmological supersymmetry breaking, and the Affleck-Dine mechanism for baryogenesis.

"Supernatural" inflation, a scenario proposed by Randall to make use of low energy supersymmetry breaking to produce a model of inflation which requires no significant fine-tuning of parameters, is described in item (2). Guth and several students have joined with Randall to analyze this model, which is rather novel both in terms of the underlying particle physics and in terms of its astrophysical consequences.

1. Supersymmetry and Cosmology

Randall and Scott Thomas (then Santa Cruz, now Stanford) considered solving the cosmological moduli problem—the overproduction of light particles in the early universe — with a brief period of inflation with Hubble constant set by the weak scale [42]. Although this model was incomplete, subsequent work by Lyth and Stewart on "Thermal Inflation" [R4] was self-consistent and incorporated many ideas from this

work.

Randall, Michael Dine (Santa Cruz), and Thomas have investigated the question of supersymmetry breaking in the early universe [10]. They showed that such supersymmetry breaking induces scalar soft potentials with curvature of order the Hubble constant.

The induced Hubble scale mass has many important consequences, including for the Affleck–Dine mechanism of baryogenesis, which requires large squark or slepton expectation values to develop along flat directions in the early universe. Randall, with Dine and Thomas, explored the implications of the Hubble scale mass and showed how the baryon to entropy ratio can be deduced in any particular model [11].

2. Supersymmetry and Cosmological Inflation

Most models of inflation require small parameters, either to guarantee sufficient inflation or the correct magnitude of the density perturbations. In "supernatural inflation," a model invented by Lisa Randall, the physics of weak-scale supersymmetry breaking is used to construct viable inflationary models in which the requisite parameters appear naturally in the form of the ratio of mass scales that are already present in the theory. Randall, M. Soljačić (undergraduate, now a graduate student at Princeton), and Alan Guth [39, 40] are studying the basic properties and predictions of this model. Inflationary models can be constructed from the flat-direction fields of a renormalizable supersymmetric potential, and such models can be realized even in the context of a simple grand-unified-theory extension of the minimal supersymmetric extension of the standard model. These models predict a very low Hubble constant during inflation, of order 10^3–10^4 GeV, a scalar density perturbation index n which is very close to or greater than unity, and negligible tensor perturbations.

A key feature of supernatural inflation, currently under investigation, is a large spike in the density perturbation spectrum at wavelengths in the vicinity of 1 Mpc. This spike is generated because supernatural models are a form of "hybrid" inflation, using two fields to achieve the inflation. One field, ψ, rolls steadily down a hill in its potential energy diagram, controlling the timing of inflation. The second field, ϕ, supplies the bulk of the energy density during inflation. Initially ϕ stays near zero, where the potential is high but is nonetheless a minimum. The coupling to the time-varying ψ field, however, causes the potential energy function to shift so that $\phi = 0$ becomes a local maximum. Classically this configuration would be an equilibrium, albeit unstable, but quantum fluctuations cause ϕ to roll off the hill of the potential energy diagram, ending inflation. This intrinsically quantum behavior invalidates the standard methods of calculating density perturbations, which treat quantum fluctuations of the scalar field as small perturbations about a well-defined classical evolution. The spike in the density perturbation spectrum arises because, when ϕ is at the maximum of its potential, the duration of inflation is very sensitive

to the occurrence of small quantum fluctuations.

Randall, Soljačić, and Guth proposed a recipe for calculating these density perturbations, but the approximations were not easy to justify [40]. Guth, Randall, and Shufang Su (graduate student) are just completing a numerical simulation, in a one-dimensional toy model, which seems to justify the key approximation. They are now attempting to use this method to investigate the details of the density perturbation spike and its consequences. A key issue is the formation of black holes, a question for which only approximate answers can be found. Several important questions remain to be investigated: (1) could such a density perturbation spike help explain the origin of the supermassive black holes that are believed to exist at the centers of many or perhaps all galaxies? (2) if the spike occurs at shorter wavelengths, could it produce primordial black holes in the solar mass range, possibly explaining the observations of the MACHO project? (3) could such a spike help to resolve the problem of slow galaxy formation encountered in mixed dark matter cosmological models?

III. B PHYSICS

The next few years should be an exciting era for b physics. Randall and Jaffe and collaborators have worked on several subjects involving b quarks. Randall and Eric Sather (graduate student) used the chiral, heavy-quark effective theory to investigate the surprisingly small SU(3) asymmetry of heavy-meson hyperfine splittings [36]. In another project Randall and Sather estimated the production rate of $BB\pi$ in e^+-e^- annihilation. They used their estimate to assess the merit of tagging B mesons for CP-violation studies by producing them together with charged pions [37].

Giovanni Bonvicini (Aleph Collaboration) and Randall [30] have shown that by studying the ratio of average neutrino energy to average electron energy in the laboratory frame, one has a sensitive probe of polarization of the Λ_b which is independent of fragmentation uncertainties. This technique should be useful for measuring the polarization, which is expected to be quite large.

Jaffe and Randall developed an approach to deep inelastic phenomena involving heavy hadrons by combining the methods of perturbative QCD with those of the heavy quark expansion [13]. This leads to a new phenomenological form for the z-dependence of the fragmentation function in which the heavy quark mass dependence is made explicit. It is then clear how to extract the maximum information which can be deduced reliably within the framework of perturbative QCD and the heavy quark expansion. Randall and Nuria Rius (postdoc, now at U. Valencia) followed up this work by explicitly incorporating the perturbative scaling, using heavy quark fragmentation into heavy hadrons to determine QCD parameters and test heavy quark symmetry [35].

On a related subject Randall and Mark Wise (CalTech) calculated an exactly

computable source of $(\Lambda/m)^2$ corrections to $B \to D^*$ decay at zero recoil [18]. This is relevant to the extraction of the Kobayashi–Maskawa matrix element V_{bc}.

Csaba Csáki (graduate student, now at UC Berkeley) and Randall [31] showed the consistency (at the $1/m$ level) of the ACCMM [R1] model and the general predictions of QCD and the heavy quark expansion. They showed at the $1/m^2$ level the model disagrees with the general result.

Randall, Zoltan Ligeti (CalTech), and Mark Wise (CalTech) analyzed uncertainties in the theoretical prediction for the inclusive $B \to X_s\gamma$ decay rate [18]. They emphasize that there is no operator product expansion for this process. Nonetheless, some nonperturbative effects involving a virtual $c\bar{c}$ loop are calculable using the operator product expansion. They give a contribution to the decay rate that involves the B meson matrix element of an infinite tower of operators. The higher dimension operators give effects that are only suppressed by powers of $m_b\Lambda_{QCD}/m_c^2 \sim 0.6$, but come with small coefficients.

IV. IMPLICATION OF EXACT SUSY GAUGE COUPLINGS FOR QCD

Lisa Randall, Ricardo Rattazzi (CERN), and Edward Shuryak (nuclear theory group sabbatical visitor and SUNY Stony Brook), studied the precise meaning of the strong interaction scale Λ in SUSY gauge theories [33]. They studied the validity of "naive dimensional analysis" and also asked whether the study of supersymmetric theories can shed light on the apparent discrepancy between the perturbative scale Λ_{QCD} and the chiral Lagrangian scale Λ_χ in QCD. In $N = 1$ supersymmetric Yang–Mills theory, naive dimensional analysis seems to work well, with Λ_χ consistently equal to the scale at which the perturbatively evolved physical coupling becomes of order 4π. They studied $N = 2$ theories to investigate the effect of instantons on the discrepancy between scales. In $N = 2$ supersymmetric SU(2) instanton corrections generate a finite ratio between the scale at which the perturbatively evolved and "nonperturbatively evolved" couplings blow up. Correspondingly, instanton effects are important even when the perturbatively evolved α is of order 1 (rather than 4π). They compared the $N = 2$ result to instanton-induced corrections in QCD, evaluated using lattice data and the instanton liquid model, and found a remarkably similar behavior.

References

[R1] G. Altarelli, N. Cabibbo, G. Corbò, L. Maiani, and G. Martinelli, *Nucl. Phys.* **B208** (1982) 365.

[R2] D. Kutasov, "A Comment on Duality in $N = 1$ Supersymmetric Non-Abelian Gauge Theories," hep-th/9606184, *Phys. Lett.* **351B** (1995) 230.
D. Kutasov and A. Schwimmer, "On Duality in Supersymmetric Yang-Mills Theory," hep-th/9505004, *Phys. Lett.* **354B** (1995) 315.

[R3] M. Berkooz, "The Dual of Supersymmetric SU($2k$) with an Antisymmetric Tensor and Composite Dualities," hep-th/9505067, *Nucl. Phys.* **B459** (1995) 513.

[R4] D.H. Lyth and E.D. Stewart, "Thermal Inflation and the Moduli Problem," hep-ph/9510204, *Phys. Rev. D* **53** (1996) 1784–1798.

Publications

[1] J. Bagger, E. Poppitz, and L. Randall, "The R-Axion from Dynamical Supersymmetry Breaking," *Nucl. Phys.* **B426** (1994) 3.

[2] J. Bagger, E. Poppitz, and L. Randall, "Destabilizing Divergences in Supergravity Theories at Two Loops," hep-ph/9505244, *Nucl. Phys.* **B455** (1995) 59–82.

[3] Z. Berezhiani, C. Csáki, and L. Randall, "Could the Supersymmetric Higgs Particles Naturally be Pseudogoldstone Bosons?" hep-ph/9501336, *Nucl. Phys.* **B444** (1995) 61–91.

[4] C. Csáki and L. Randall, "Phenomenological Constraints on the Higgs as Pseudo-Goldstone Boson Mechanism in Supersymmetric GUT Theories," MIT-CTP-2478, hep-ph/9512278, *Nucl. Phys.* **B466** (1996) 41–59.

[5] C. Csáki, L. Randall, and W. Skiba, "Dynamical Supersymmetry Breaking," MIT-CTP-2532, hep-th/9605108, *Nucl. Phys.* **B479** (1996) 65–81.

[6] C. Csáki, L. Randall, W. Skiba, "Composite Intermediary and Mediator Models of Gauge Mediated Supersymmetry Breaking," MIT-CTP-2654, hep-ph/9707386, *Phys. Rev. D* **57** (1998) 383–390.

[7] C. Csáki, L. Randall, and W. Skiba, "More Dynamical Supersymmetry Breaking," MIT-CTP-2532, hep-th/9605108, *Nucl. Phys.* **479** (1996) 65–81.

[8] C. Csáki, L. Randall, W. Skiba, and R.G. Leigh, "Supersymmetry Breaking Through Confining and Dual Theory Gauge Dynamics," MIT-CTP-2543, hep-th/9607021, *Phys. Lett.* **B387** (1996) 791–795.

[9] I. Dasgupta, B.A. Dobrescu, and L. Randall, "Vacuum Instability in Low-Energy Supersymmetry Breaking Models," BUHEP-96-25, hep-ph/9607487, *Nucl. Phys.* **B483** (1997) 95–110.

[10] M. Dine, L. Randall, and S. Thomas, "Supersymmetry Breaking in the Early Universe," hep-ph/9503303, *Phys. Rev. Lett.* **75** (1995) 398–401.

[11] M. Dine, L. Randall, and S. Thomas, "Baryogenesis from Flat Directions of the Supersymmetric Standard Model," hep-ph/9507453, *Nucl. Phys.* **B458** (1996) 291–326.

[12] J. Erlich, A. Naqvi, and L. Randall, "The Coulomb Branch of N=2 Supersymmetric Product Group Theories from Branes," MIT-CTP-2707, hep-th/9801108.

[13] R.L. Jaffe and L.J. Randall, "Heavy Quark Fragmentation into Heavy Mesons," *Nucl. Phys.* **B412** (1994) 79.

[14] E. Katz, L. Randall and S. Su, "Supersymmetric Partners of Oblique Corrections," MIT-CTP-2646, hep-ph/9706478, *Nucl. Phys.* Proc. Suppl. **B62** (1998) 299–303.

[15] E. Katz, L. Randall and S. Su, "Supersymmetric Partners of Oblique Corrections," MIT-CTP-2708, hep-ph/9801416.

[16] R.G. Leigh, L. Randall, and R. Rattazzi, "Unity of Supersymmetry Breaking Models," ILL-TH-97-1, hep-ph/9704246, *Nucl. Phys.* **B501** (1997) 375–408.

[17] L. Lellouch, L. Randall and E. Sather, "The Rate for $e^+ e^- \longrightarrow B B^{\pm} \pi^{\mp}$ and Its Implications for the Study of CP-Violation, B_s Identification, and the Study of B Meson Chiral Perturbation Theory," *Nucl. Phys.* **B405** (1993) 55–79.

[18] Z. Ligeti, L. Randall, and M.B. Wise "Comment on Nonperturbative Effects in $\bar{B} \to X_s \gamma$," CALT-68-2097, hep-ph/9702322, *Phys. Lett.* **B402** (1997) 178–182.

[19] A. E. Nelson and L. Randall, "Naturally Large $\tan\beta$," *Phys. Lett.* **B316** (1993) 516–520.

[20] E. Poppitz and L. Randall, "The '3-1' Model: The Minimal Model of Calculable Dynamical Supersymmetry Breaking," hep-ph/9411295.

[21] E. Poppitz and L. Randall, "Low Energy Kähler Potentials in Supersymmetric Theories With (Almost) Flat Directions," hep-th/9407185, *Phys. Lett.* **336B** (1994) 402.

[22] E. Poppitz and L. Randall, "Holomorphic Anomalies and the Nonrenormalization Theorem," EFI-96-32, hep-th/9608157, *Phys. Lett.* **B389** (1996) 280–286.

[23] L. Randall, "ETC with a Gim Mechanism," *Nucl. Phys.* **B403** (1993) 122–140.

[24] L. Randall, "The Inclusive Semileptonic B Decay Lepton Spectrum from $B \to Xe\bar{\nu}$," hep-ph/9407300, proceedings of the WHEPP-3 Phenomenology Workshop, *Pramana* **45** (1995) S255–S262.

[25] L. Randall, "Flat Directions in Supersymmetric Theories," presented at 30th Rencontres de Moriond: *Electroweak Interactions and Unified Theories,* Meribel les Allues, France, 11-18 Mar 1995, MIT-CTP-2452, hep-ph/9507266..

[26] L. Randall, "New Mechanisms Of Gauge Mediated Supersymmetry Breaking." MIT-CTP-2591, hep-ph/9612426, *Nucl. Phys.* **B495** (1997) 37–56.

[27] L. Randall, "Models of Dynamical Supersymmetry Breaking," MIT-CTP-2652, hep-ph/9706474.

[28] L. Randall, "New Mechanisms of Gauge Mediated Supersymmetry Breaking," MIT-CTP-2653, hep-ph/9706475. *Les Arcs, Electroweak interactions and unified theories** (1997) 227–233.

[29] L. Randall, "Supersymmetry and Inflation," MIT-CTP-2699, hep-ph/9711471, to appear in *Perspectives on Higgs Physics II, edited by G.L. Kane, World Scientific, Singapore.*

[30] L. Randall and G. Bonvicini, "Optimized Variables of the Study of Λ_b Polarization," *Phys. Rev. Lett.* **73** (1994) 392.

[31] L. Randall and C. Csáki, "The ACCMM Model and the Heavy Quark Expansion," *Phys. Lett.* **B324** (1994) 451-460.

[32] L. Randall and C. Csáki, "The Doublet-Triplet Splitting Problem and Higgses as Pseudo-Goldstone Bosons," presented at PASCOS/HOPKINS 1995, Baltimore, MD, Mar 22-25, 1995, and at SUSY '95, Palaiseau, France, May 15-19, 1995, MIT-CTP-2460, hep-ph/9508208.

[33] L. Randall, R. Rattazzi and E. Shuryak "Implication of Exact Susy Gauge Couplings for QCD," CERN-TH98-63, hep-ph/9803258.

[34] L. Randall and N. Rius, "Why a Scalar Explanation of the L3 Events is Implausible," *Phys. Lett.* **B309** (1993) 365–370.

[35] L. Randall and N. Rius, "Using Heavy Quark Fragmentation into Heavy Hadrons to Determine QCD Parameters and Test Heavy Quark Symmetry," MIT-CTP-2257, hep-ph/9405217, *Nucl. Phys.* **B441** (1995) 167–196.

[36] L. Randall and E. Sather, "Heavy Meson Hyperfine Splittings: A Puzzle for Heavy Quark Chiral Perturbation Theory," *Phys. Lett.* **B303** (1993) 345–349.

[37] L. Randall and E. Sather, "The Rate for $B\overline{B}$ Production Accompanied by a Single Pion and Its Implications for the Study of CP Violation," MIT-CTP-2214, proceedings of 1993 Rencontres de Moriond.

[38] L. Randall and E. Sather, "The QCD Scale in the Heavy Quark Expansion," MIT-CTP-2167, *Phys. Rev. D* **49** (1994) 6236–6239.

[39] L. Randall, M. Soljačić, and A.H. Guth, "Supernatural Inflation," MIT-CTP-2499, hep-ph/9601296.

[40] L. Randall, M. Soljačić, and A.H. Guth, "Supernatural Inflation: Inflation from Supersymmetry with No (Very) Small Parameters," MIT-CTP-2501, hep-ph/9512439, *Nucl. Phys.* **B472** (1996) 377–408.

[41] L. Randall and R. Sundrum, "$B \to s\gamma$ and $B_s \to \mu^+\mu^-$ in Extended Technicolor Models," *Phys. Lett.* **B312** (1993) 148–154.

[42] L. Randall and S. Thomas, "Solving the Cosmological Moduli Problem with Weak Scale Inflation," MIT-CTP-2331, hep-ph/9407248, *Nucl. Phys.* **B449** (1995) 229–247.

[43] L. Randall and M. Wise, "Chiral Perturbation theory for $B \to D^*$ and $B \to D$ Semileptonic Transition Matrix Elements at Zero Recoil," *Phys. Lett.* **B303** (1993) 135–139.

[44] T. Wynter and L. Randall, "Constraints on a Massive Dirac Neutrino Model," MIT-CTP-2212, *Phys. Rev. D* **50** (1994) 3457–3467.

Invited Talks

1. L. Randall, "ETC wth a GIM Mechanism," Aspen Center for Physics (January & March 1993).

2. L. Randall, "The Rate for $B\overline{B}$ Production Accompanied by a Single Pion and Its Implications for the Study of CP Violation," Rencontres de Moriond (March 1993).

3. L. Randall, invited talk given at WHEPP-3 Phenomenology Workshop, Madras, India (January 1994).

4. L. Randall, "The Doublet-Triplet Splitting Problem and the Higgses as Pseudogoldstone Bosons," SUSY 95, International Workshop on *Supersymmetry and Unification of Fundamental Interactions*, Ecole Polytechnique, Paliseau, France (May 1994).

5. L. Randall, invited talk given at Joint US-Polish Workshop, *Physics from the Planck to the Electroweak Scale,* Warsaw, Poland (September 1994).

6. L. Randall, "The Doublet-Triplet Splitting Problem and the Higgses as Pseudogoldstone Bosons," PASCOS Symposium, Johns Hopkins University (Joint Meeting of the International Symposium on Particles, Strings, and Cosmology), Baltimore, MD (March 1995).

7. L. Randall, "Supernatural Inflation," ITP Conference on Unification: *From the Weak Scale to the Planck Scale*, Institute for Theoretical Physics, Santa Barbara (September 1995).

8. L. Randall, "Super Cosmology and Superior Cosmology," KOSEF-JSPS Winter School, *Recent Developments in Particle and Nuclear Theory*, Seoul, Korea (February, 1996).

9. L. Randall, "Dynamical Supersymmetry Breaking," SUSY '96, Fourth International Conference on Supersymmetries in Physics, College Park, MD (June 1996).

10. L. Randall, "Standard Model and Beyond," Tbilisi, Georgia (August 1996).

11. L. Randall, "Dynamical Supersymmetry Breaking," Strongly Coupled Gauge Theories, Nagoya (November 1996).

12. L. Randall, "New Mechanisms for Gauge-Mediated Supersymmetry Breaking," Electroweak Session, Moriond 97 (March 1997).

13. L. Randall, "Dynamical Supersymmetry Breaking," Research Workshop of the Israel Science Foundation on Dept. of Particle Physics at the Weizmann Institute of Science (April 1997).

Theses Supervision

1. Csaba Csáki, "Beyond the Minimal Supersymmetric Standard Model," Ph.D., May 1997 (L. Randall, supervisor).

2. Minjoon Kouh, "Arrays of Quantum Dots as Semiconductors," S.B., May 1997 (L. Randall, supervisor).

3. Serna, Mario, "Day-night and energy dependence of MSW solar neutrinos for maximal mixing," M.S., May 1999 (L. Randall, supervisor).

4. Witold Skiba, "Strong Dynamics in Theories Beyond the Standard Model," Ph.D., May 1997 (L. Randall, supervisor).

5. Marin Soljačić, "Supernatural Inflation: Inflation from Supersymmetry with No (Very) Small Parameters," S.B., May 1996 (L. Randall, supervisor).

6. Thomas Wynter, "A Model of Massive Neutrinos," S.M., May 1993 (L. Randall, supervisor).

FINAL TECHNICAL REPORT: AXION OJI

Leslie J Rosenberg
MIT-Laboratory for Nuclear Science.
November 1999

1. Introduction and overview of the RF cavity axion program

The nature of the dark matter in the Universe is one of the pre-eminent problems in all of science. The case for a large non-baryonic component has only been strengthened by the recent dramatic developments in experimental cosmology. A prime Cold Dark Matter (CDM) candidate is the axion, which arises from an elegant and minimal extension of the Standard Model to enforce Strong-CP conservation. Sikivie showed how dark-matter axions, long thought to be 'invisible', could be detected by their conversion to a weak microwave signal in a strong magnetic field, resonantly enhanced by a high-Q cavity.

The work of Sikivie and others prepared the way for our large-scale RF cavity axion search now operating since early 1996 (a collaboration largely of MIT and LLNL, also with important contributions from U of Florida, Fermilab/Chicago and LBNL). This experiment reached the sensitivity required to see KSVZ axions, one of two benchmark models, for the first time and has operated (and continues to operate) at >90% duty factor for over three years, starting with its very first commissioning run.

Selected R&D across many fronts targeted at increasing sensitivity and scan rate has been successful, and we are now positioned to carry out a much more significant experiment, one that could detect the more generic DFSZ axion, even should they constitute only 50% of the CDM density of our halo. One particular emphasis of the OJI support, especially in the early development of the RF cavity search, was the characterization and construction of UHF through S-band resonators to quickly determine microwave surface resistance of materials and effects of surface treatments. Optimizing the surface resistance gives higher Q, and higher Q directly translates into higher axion signal.

Brief Overview of the Evidence for Cold Dark Matter

The evidence that the Universe contains a significant component of dark matter is direct and unassailable. Dynamical estimates of the mass of large clusters of galaxies and estimates of their mass from their gravitational lensing of background quasars are consistent with one another, and give the value $\Omega_{clu}=0.3\pm0.1$. Studies of the peculiar velocities of galaxies on the largest scales imply $\Omega_{mat}\sim0.4$ to 2. Over the last two years, two independent surveys of high red-shift Type Ia supernovae have reported results which imply $\Omega_{mat}=0.25\pm0.05$ when the condition of a flat Universe ($\Omega_{mat} + \Omega_\Lambda = 1$) is imposed on the fit to the data. The key point is that, while Ω_{mat} may be less than unity, it cannot be smaller than 0.2, and certainly not as small as 0.1.

On the other hand, nucleosynthesis requires that the baryonic component of the Universe satisfy $\Omega_{bar}\, h^2 = 0.019\pm0.001$. This constraint has recently become far more restrictive because good measurements of the primordial deuterium-to-hydrogen ratio from quasar-

backlit Lyman absorption spectra have finally been made. Moreover, the value of the Hubble constant has become far better known: $h = 0.65 \pm 0.10$. The dark matter of the Universe could only be completely baryonic for $h \sim 0.3$ or less, which is inconsistent with all measurements.

The nucleosynthesis constraint also implies that some baryons are dark since the luminous matter of the universe only contributes $\Omega_{vis} \sim 0.005$, whereas Ω_{bar} is greater than 0.03. Hence there are at least two dark-matter problems: (i) Where are the dark baryons? (ii) What is the dark matter that makes up 90% of the Universe? Our axion search addresses the second problem. The overall situation is depicted in Figure 1.

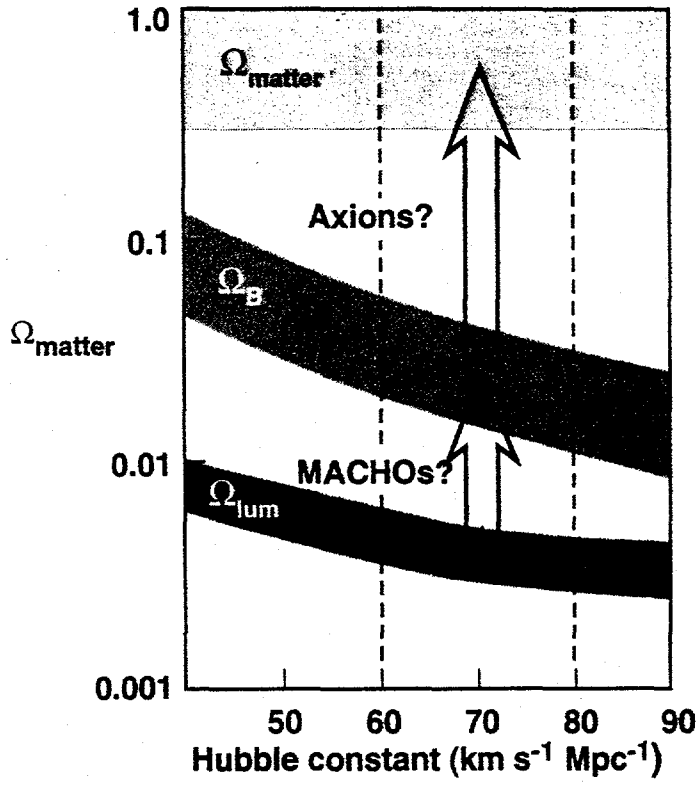

Figure 1. Summary of the dark-matter problem.

The leading dark-matter candidates are collisionless particles, specifically neutrinos, axions and weakly interacting massive particles (WIMPs). Neutrinos are called hot dark matter (HDM) because they have large primordial dispersion from the point of view of structure formation, whereas axions and WIMPs are cold dark matter (CDM) because their primordial velocity dispersion is negligible. Consistency to all observed structure in the Universe, from optical surveys of the distribution of galaxies on the smallest scales to measurements of the cosmic microwave background anisotropies on the largest, always require a significant CDM component ($\Omega_{cdm} \sim 0.45$ to 0.70). In addition, they may be a smoothly distributed vacuum energy ($\Omega_\Lambda \sim 0$ to 0.5), and perhaps a small HDM component ($\Omega_{hdm} \sim 0$ to 0.2). The recent Super-Kamiokande atmospheric neutrino

oscillation data imply a negligible Ω_{hdm} in both ν_μ and ν_τ unless their masses are, for some reason, essentially degenerate.

CDM falls into the gravitational potential wells of galaxies and thus contributes to the dark-matter density in galactic halos. In fact it is the CDM density perturbations which seed such structures in the first place. The maximum likelihood estimate of our local CDM density, based on all galactic observables (rotation curve, projected disk density, microlensing optical depth), is $\rho_{cdm}=7.5\times10^{-25}$g/cc (~ 450 MeV/cc). Also, since CDM particles are dissipationless, their spectrum may possess fine structure, reflecting the infall and oscillation of CDM particles across the growing halo. Being able to see very narrow lines not only increases the discovery potential of the experiment, but also, should the axion be found, provides a detailed history of the evolution of the galaxy.

Particle Physics of the Axion

The axion was postulated two decades ago to explain why QCD conserves the discrete symmetries P and CP in spite of the fact that the Standard Model as a whole violates those symmetries. It is the quasi-Nambu-Goldstone boson associated with the spontaneous breakdown of the $U_{PQ}(1)$ symmetry proposed by Peccei and Quinn. The properties of the axion depend mainly on one unknown parameter, the PQ symmetry-breaking scale f_A. Both the mass of the axion and its couplings to normal matter and radiation are inversely proportional to f_A with $m_A \approx 0.6\text{eV}\ (10^7\text{GeV} / f_A)$. Central to this experiment is the coupling of the axion to two photons:

$$\mathcal{L} = -g_{a\gamma\gamma}\phi_A \mathbf{E}\cdot\mathbf{B},$$

where ϕ_A is the axion field and the dimensioned coupling is $g_{A\gamma\gamma}$. The coupling can be written in terms of a dimensionless model-dependent number of order one, viz.,

$$g_{A\gamma\gamma} = (\alpha\, g_\gamma / \pi\, f_A).$$

For KSVZ axions, $g_\gamma \sim 0.97$ whereas for DFSZ axions , $g_\gamma \sim -0.36$.

Originally it was thought that f_A would be the electroweak scale, ~250 GeV, implying a heavy axion, $m_A \sim \vartheta(100\text{ keV})$ and couplings strong enough to permit its detection in conventional experiments using accelerators and reactors. But that heavy axion was quickly ruled out, and models were constructed that allowed f_A in principle to be anywhere up to the Planck scale, in which case the axion couplings are enormously suppressed. However, even though axions are very weakly coupled in these models, they turned out to be severely constrained by astrophysical and cosmological considerations. As a result of these constraints, the present open window for the axion mass is approximately $10^{-6} < m_A < 10^{-2}$ eV. The upper limit comes from a seamless overlap of stellar evolution limits, starting with that from SN1987a, and ultimately connecting with accelerator-based limits in the keV range. Cosmology sets the lower mass limit. Generically, the axion mass density of the Universe increases with decreasing m_A. Axions produced by the vacuum-misalignment mechanism provide the critical density for closing the Universe if the axion mass is in the 10^{-6} to 10^{-5} eV range, where our present experiment searches. There could also be a contribution from string radiation. The key

point is that the lower mass range 10^{-6} to 10^{-5} eV is prime territory to begin the search, corresponding as it does to $\Omega_A \sim \vartheta(1)$.

2. Present Experiment Description

Axions constituting our galactic halo are a cold dense Bose fluid; for μeV masses, their local number density would be $\vartheta(10^{14}$ /cc). Furthermore, from galactic dynamics the axion's virial velocity should be ~270 km/sec implying a small broadening of its spectrum above its rest mass with a width of $\Delta E/m_A \sim 10^{-6}$. Its very small momentum also implies a very long de Broglie wavelength, $\lambda \sim 100$ m. In 1983, Pierre Sikivie published a concept for an experiment by which such galactic axions could be detected by a Primakoff interaction. Specifically, as the axion has a two-photon coupling, it can be stimulated to decay into a single real photon carrying its full energy (mass + kinetic) in the presence of an external magnetic field, and furthermore the rate can be resonantly enhanced in a microwave cavity. In spite of the prodigious density of axions, the expected signal would still be extraordinarily weak, the conversion power being given by:

$$P_{lmn} = \left(\frac{\alpha}{\pi} g_\gamma \frac{1}{f_A}\right) B_0^2 V \rho_A C_{lmn} \frac{1}{m_A} Q_L$$

where B_0, V are the strength and volume of the magnetic field, Q_L the loaded (outcoupled) quality factor of the microwave cavity ~10^5, and C_{lmn} the form factor for a particular mode of the cavity; this latter factor expresses the overlap of the cavity mode E-field with the magnet's B-field, and is a number of order unity for the mode of interest, TM_{010}. For the present experiment, and for KSVZ axions, $P \sim 5\times10^{-22}$ Watts.

Since we don't know where in frequency the axion would appear, the cavity must be tuned. At each central frequency of the cavity, the power spectrum is integrated for a time long enough such that the noise fluctuations will average away, leaving the axion signal at a desired signal-to-noise ratio (s/n). The essence of the search strategy is Dicke's radiometer equation $s/n = (P_{sig} / k_b T_s) (t/BW)^{1/2}$ where P_{sig} is the expected signal power, BW its expected bandwidth, $T_s = T_n + T$ the system noise temperature, and t the integration time. Up to where non-statistical processes become important, the s/n is improved by making the signal stronger, reducing the noise power, or integrating longer. In practice, the integration time at each frequency is set by our goal of covering a certain mass range at a certain sensitivity within a given time, *e.g.,* one decade at KSVZ axion sensitivity in three years.

Our present collaboration (MIT, LLNL, Florida, LBNL, FNAL) constructed and operated a large-scale dark-matter axion experiment which for the first time reached sensitivity to KSVZ axions, where it continues to scan in the 1.3-13 μeV range. This experiment built upon the experience and personnel of two small first-generation experiments which identified some of the key challenges and developed essential technologies. Those earlier experiments however fell 100—1000 short in power sensitivity to see halo axions of KSVZ or DFSZ couplings.

Figure 2 is a diagram of the apparatus. The 8 tesla magnet is slightly over 50 cm diameter and 100 cm long, accommodating one or more cylindrical microwave cavities; these are made of stainless steel plated with high purity copper. The single cavity Q~250,000 is the theoretical maximum, limited by the copper anomalous skin depth. The cavities are tuned by radially translating copper ($\Delta f>0$) or ceramic ($\Delta f<0$) tuning rods between the wall and center of the cavity. These rods can be moved reproducibly in steps of a few hundred nanometers, or ~2 kHz shift in resonant frequency.

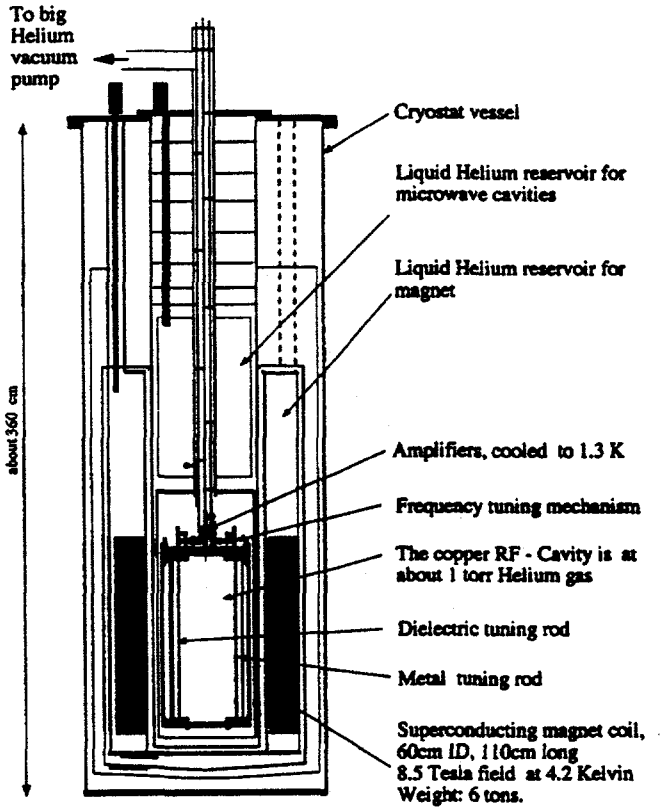

Figure 2. Diagram of the present apparatus.

The detector is essentially an exquisitely sensitive radio receiver, with the cavity as an input tank circuit (Figure 3). An antenna of adjustable insertion depth couples power from the cavity to the first- and second-stage amplifiers cooled to near the cavity temperature, T~1.3 K. These are high-electron mobility transistor (HEMT) amplifiers built by NRAO, characterized by a noise temperature T_n~4.6 K at the beginning of data-taking (but recently substantially improved), gain of 17 dB, and reflection coefficient from the input of about -30 dB.

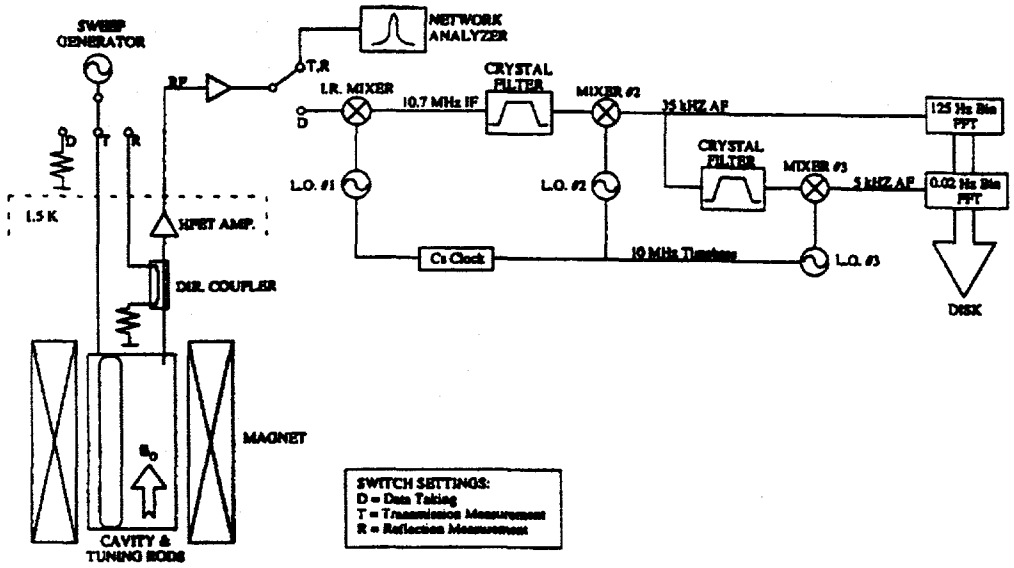

Figure 3. Schematic diagram of the receiver.

After 35 dB of further amplification at room temperature, the signal is down-converted to 10.7 MHz by an image-rejection mixer. An eight-pole crystal filter sets a 30 kHz measurement bandwidth and prevents image power from entering the second mixing stage. The signal is down-converted a second time, in effect shifting the cavity resonant frequency to 35 kHz. A commercial fast Fourier transform (FFT) spectrum analyzer generates the "medium-resolution" power spectrum (this is the main data channel). During each 80-sec run, 10,000 subspectra are measured and averaged, resulting in a 400 point, 125 Hz/point power spectrum. This resolution is well matched to a search for the Maxwellian component of the halo, ~750 Hz wide (~6 spectrum channels wide). Additionally, the receiver analog output is applied to a six-pole filter and a third mixing stage, centering the resonant frequency at ~5 kHz. A commercial ADC/DSP PC module generates one 250,000 point 0.02 Hz/point power spectrum from a 60-sec interval within each run (without averaging). This is well matched to search for the predicted fine structure with fractional width down to ~ $\vartheta(10^{-11})$.

After every 80 seconds, the cavity frequency f_0 is tuned upwards by 2 kHz, the cavity and environmental parameters recorded, and another spectrum acquisition initiated. After each frequency range is swept out in this way, at least two more sweeps are made over the same range, usually separated by a few weeks. Thus each frequency is covered in at least 45 subspectra. During off-line processing, the middle 200 frequency bins of each 400-point spectrum are gain-corrected by the receiver response, leaving a residual slow variation with frequency across the spectrum by ~1 dB. A five-parameter equivalent circuit model removes this variation, leaving a flat, corrected spectrum. The subspectra are then linearly combined with a weighting function that accounts for the B_0, T, C, Q and $f\text{-}f_0$ for each. For our first published results, this resulted in a single spectrum of 10^6 points between 701-800 MHz.

3. Results of DOE support

Figure 4(left) shows the expected signal from KSVZ axions, and the noise background for axions of six- and one-channel width. Figure 4(right) shows the deviation of the single channel power from the thermal mean for all of the data taken. Candidate peaks are those one- (six-) channel fluctuations with 3.3σ ($2.25\times6^{1/2}\sigma$) power excess, resulting in 538 (6535) candidates. These candidates were rescanned leaving 6 (23) persistent candidates. Further investigation showed all persistent candidates were due to external interference.

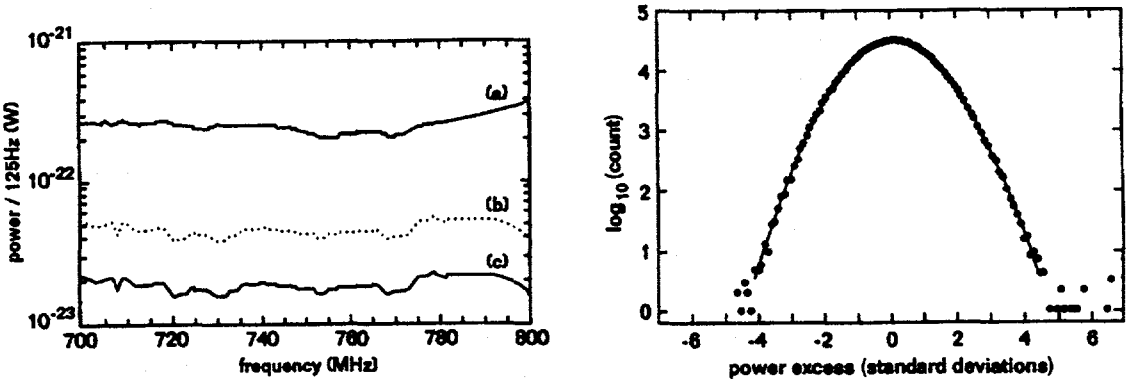

Figure 4. Left: (a) Expected KSVZ signal power, (b) Noise background for axion six channels wide, (c) Noise background for axion one channel wide. Right: Distribution of the deviation of single channel noise power from the thermal mean, in intervals of 0.1σ, for a 100 MHz frequency span.

Figure 5 shows the axion couplings and masses excluded at 90% c.l. in our last Physical Review Letter for axions with the expected Maxwellian velocity distribution,[1] along with the KSVZ and DFSZ model predictions. Also shown on the inset are the regions excluded by the first-generation microwave cavity experiments of Rochester-BNL-FNAL and Florida. This experiment is more than two orders of magnitude more sensitive, and is the first to exclude a standard axion model (KSVZ) over any mass range. The high-resolution channel is analyzed similarly. The power spectra are binned on-line at 0.02, 0.16 and 1.3 Hz, for which candidates are defined as those peaks with more than 15σ, 8σ and 5σ excess power respectively. After rescanning candidate peaks and eliminating external noise sources, no candidates remained, resulting in upper limits near 3.3×10^{-23} W, 5.0×10^{-23} W and 8.8×10^{-23} W respectively. Furthermore, we searched for coincidences between medium- and high-resolution candidates, and after excluding obvious RF sources, found none.

---

1 C. Hagmann et al., Phys. Rev. Lett. **80**, 2043(1998).

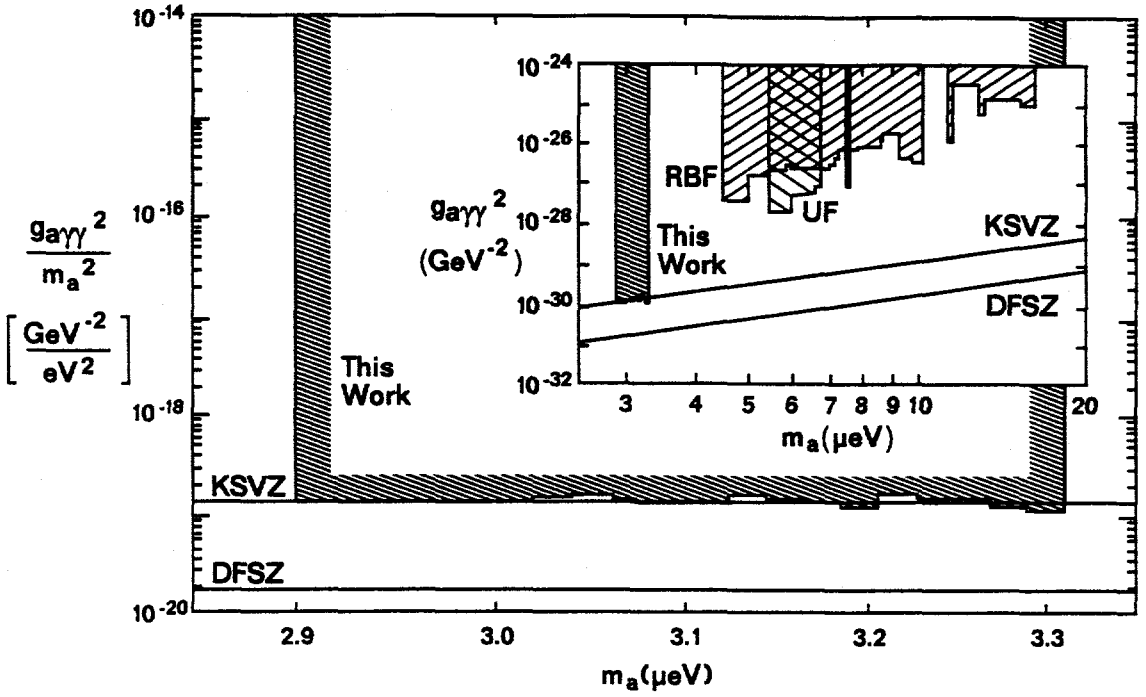

Figure 5. Axion couplings and masses excluded at the 90% c.l. by this experiment. Also shown are KSVZ and DFSZ model predictions, and regions excluded by earlier microwave cavity experiments. All results are scaled to $\rho_A = \rho_{halo} = 0.45$ GeV/cc.

Data-taking has continued uninterruptedly since publication of the 1998 Physical Review Letter, with the range 600—810 MHz (2.50—3.35 μeV) and the range down to 520 MHz (2.2 μeV) now complete at the same level of sensitivity. The first 100 MHz data sample took about 3 years to acquire, this last 100 MHz data sample took about 1 year to acquire. This speedup came from improvements in our HEMT cryogenic amplifiers. We started data-taking with amplifiers having noise temperature of 4.6 K, the most recent HEMT amplifiers have noise temperature better than 1.5 K. All the 4-cavity hardware has been fabricated, and the piezoelectric actuators (discussed later) developed for data-taking starting next month in the 1-2 Ghz range. At the moment, the experiment is fitted with a single cavity and a single large ceramic rod; we will spend the next few weeks to understanding the behavior of the system with dielectric rod tuning and then begin exploring frequencies in the 360—450 MHz (1.04—1.87 μeV) range.

Result of Cavity R&D Activity

The key elements of the RF cavity axion detector are the magnet, high Q cavity, and low noise amplification. The sensitivity of the experiment improves with increasing cavity Q, so long as the Q line-width does not get narrower than the axion line-width. It is therefore crucial that the axion detection cavity has wall RF surface resistance as low as possible. To this end, we made compact stripline TEM resonators in order to determine the surface resistance of various materials. The initial interest of the study was gross characterization of materials, but later we used the technique to characterize various

plating and surface treatments with figure-of-merit the lowest possible RF surface resistance. Much of the description following is from the MIT-UROP thesis of Darin Kinion from his work in our axion search group.

A stripline resonator is a planar transmission line structure consisting of a thin conducting sandwich between two slabs of dielectric, all sandwiched between ground planes. This geometry is shown in Fig. 6 (upper). The geometry of the thin central conductor is shown in Fig. 6 (lower). Here, microwave power is incident from the left, and the transmitted power exits to the right.

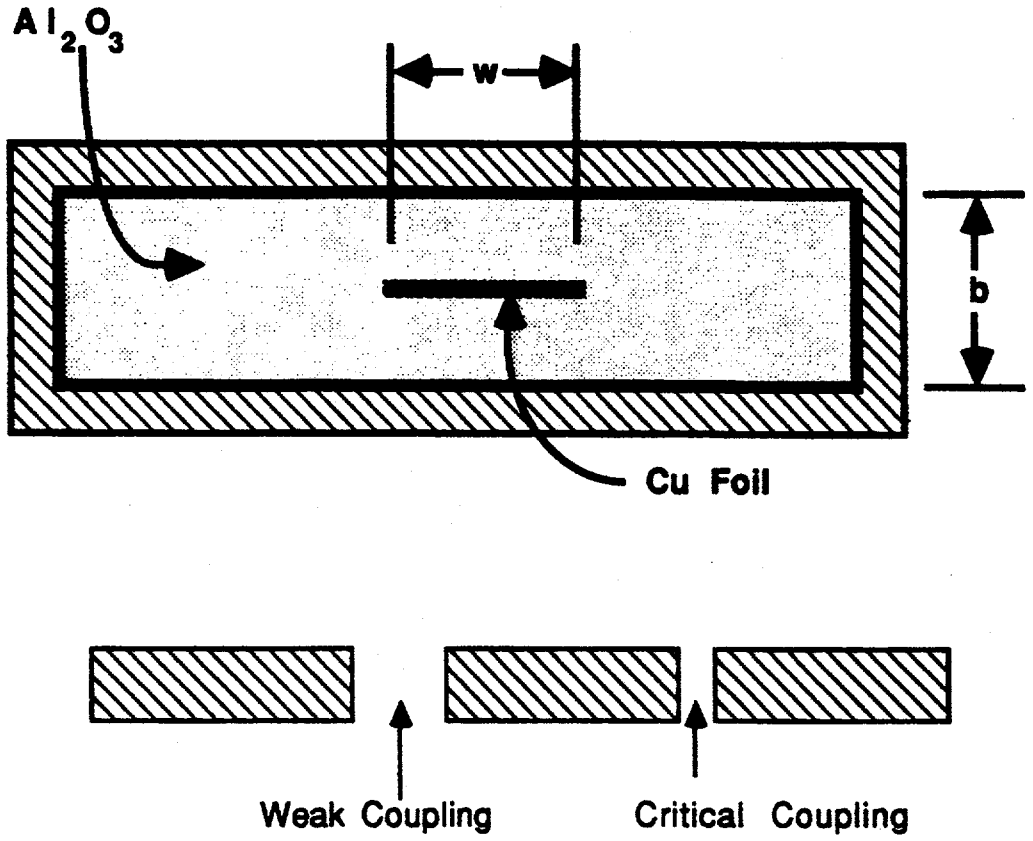

Figure 6. Upper: Cross section of the centered stripline. The thickness of the center conductor (here copper) is 0.1 mm. Lower: Geometry of the center conductor.

Formulas have been developed from purely empirical fits to data. These have been found to give reasonable agreement with the characteristic stripline impedance and attenuation. For the geometry used by our axion search group, the transverse dimensions of the center conductor are small compared to the other transverse dimensions of the resonator. So, to a good approximation, the characteristic impedance is given by

$$Z_0(Ohms) = \frac{30\pi}{\sqrt{\varepsilon_r}} \frac{b}{w + 0.441b}$$

For our work, $\sqrt{\varepsilon_r} = 3.033$, b=16mm, w=3.24mm, hence Z_0=50 Ω. A resonator proper is formed by making gaps in the center conductor. The input and output signals are then capacitively coupled into the resonator. One way to model the gaps is by a three capacitor equivalent circuit, as shown in Fig. 7.

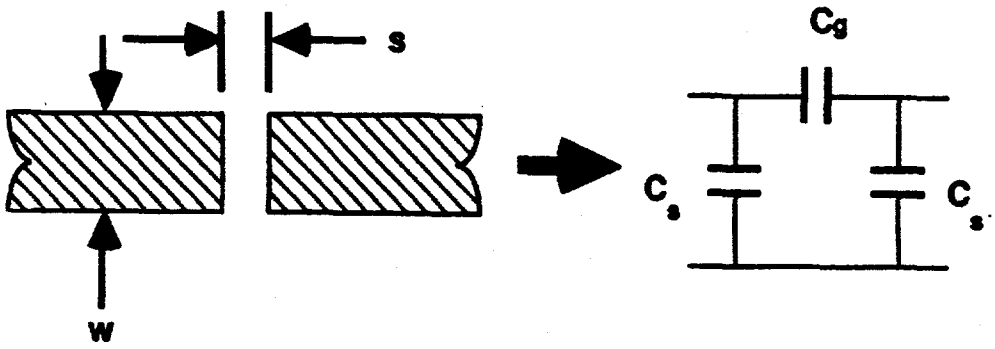

Figure 7. An equivalent three capacitor model for a gap of width s in a stripline. C_g is the gap capacitance, and C_s is the shunt capacitance.

The capacitor values in this equivalent circuit model are

$$C_g = \frac{1}{4\pi Z_o f}\left[\frac{1+(2Z_oB_b+Z_oB_a)\cot(\frac{\pi s}{\lambda_g})}{\cot(\frac{\pi s}{\lambda_g})-(2Z_oB_b+Z_oB_a)}\right]-\frac{B_a}{4\pi f} \quad F$$

$$C_s = \frac{Y_o+B_a\cot(\frac{\pi s}{\lambda_g})}{2\pi f[\cot(\frac{\pi s}{\lambda_g})-\frac{B_a}{Y_o}]} \quad F$$

where

$$B_a = \frac{-2b}{\lambda_g}\ln\left[\cosh(\frac{\pi s}{2b})\right]$$

$$B_b = \frac{b}{\lambda_g}\ln\left[\coth(\frac{\pi s}{2b})\right]$$

The value of the gap capacitance is a strong function of gap width, making it difficult to cut a gap width to yield a particular capacitance value. These formulae are useful for estimating, but in the end we cut the gap widths by trial and error. At critical coupling, half the resonator power is dissipated in the external circuitry (c.f., Fig. 8). Of course, at resonance, the impedance looking into the resonator is purely real. The gap width is adjusted until the input impedance is 50Ω at resonance via a network analyzer reflection measurement. The resonance is at the "shunt-detuned" frequency where the slight coupling capacitive impedance is cancelled by a small shift in resonant frequency.

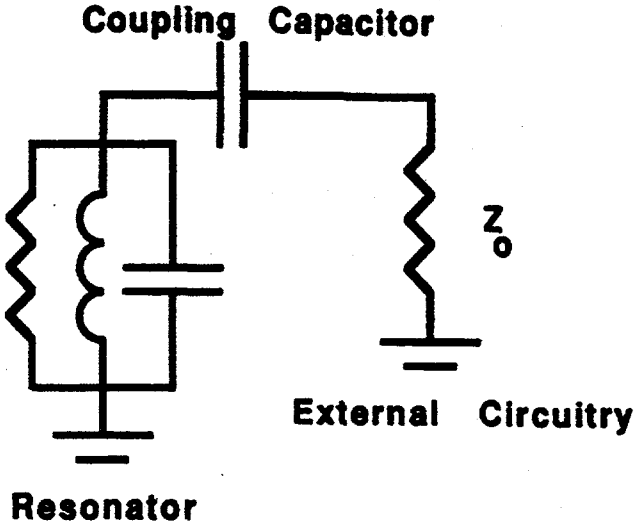

Figure 8. Circuit model for the stripline resonator. The source of microwave power is not shown; it is very weakly-coupled into the resonator.

We use two relations to extract the surface resistance of the center conductor material from the unloaded Q. The first relation relates Q to the attenuation coefficient, the length where the power is attenuated by a factor 1/e.

$$Q = \frac{\beta}{2\alpha} \text{ where } \beta = \frac{2\pi f\sqrt{\varepsilon_r}}{c}.$$

The total attenuation coefficient is the sum of losses in the dielectric and conductor $\alpha = \alpha_d + \alpha_c$. The dielectric attenuation in the TEM mode depends only on the dielectric and is given by

$$\alpha_d = \frac{2\pi f\sqrt{\varepsilon_r}}{c}\tan\delta \text{ where } \delta \text{ is the dielectric loss tangent.}$$

The second relation is between the conductor loss and surface resistance

$$R_s = \frac{Z_0 b}{0.16\alpha_c B} \text{ where the geometric factor is given by}$$

$$B = 1 + \frac{1}{0.5w + 0.7t}\left(0.5 + \frac{0.414t}{w} + \frac{1}{2\pi}\ln\left[\frac{4\pi w}{t}\right]\right)$$

Combining these expressions gives the surface resistance in terms of Q, Z_0, and the geometry of the resonator

$$R_s = \frac{z_0 b\pi f_0}{0.16Bc}\left[\frac{\sqrt{\varepsilon_r}}{Q} - \tan\delta\right]$$

The shell of the resonator (acting as ground planes) was constructed from OFHC copper. It consists of a cylindrical body with two removable flat plates. SMA connectors are fitted to seats on opposite sides of the body, a wire from the center conductor extends inside the shell. The dimensions of the resonator are shown in Fig. 9. The dielectric is

aluminum oxide (AL-23 material from Johnson-Matthey) in the form of disks, with the same inner radius as the cylindrical body and half the height. Two such disks almost completely fill the inside of the resonator. The inner conductor usually was thin foils with thickness usually 0.1mm and width 3.24mm. The center foil conductor connects to the SMA center pin with thin wire and conducting epoxy. The end caps were then bolted onto the body forming a transmission line. Gaps were eventually made in the foils creating a resonant structure.

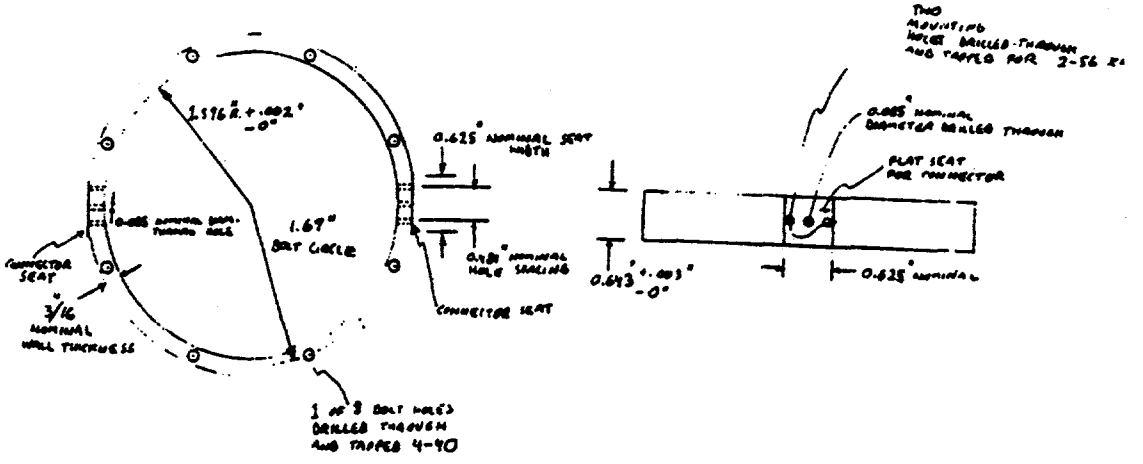

Figure 9. Shell dimensions of the resonator.

The characteristic impedance of the transmission line structure was determined by measuring the impedance with one end shorted, then opened, and combining them according to

$$z_0 = \sqrt{Z_{in}Z_{short} * Z_{in}Z_{open}}$$

We mostly worked at frequencies between 2.2 and 2.7GHz. Both sets of measurements were corrected for the electrical lengths of cables and the second set was also corrected for the length of the short. Typical results of these measurements are shown in Fig. 10.

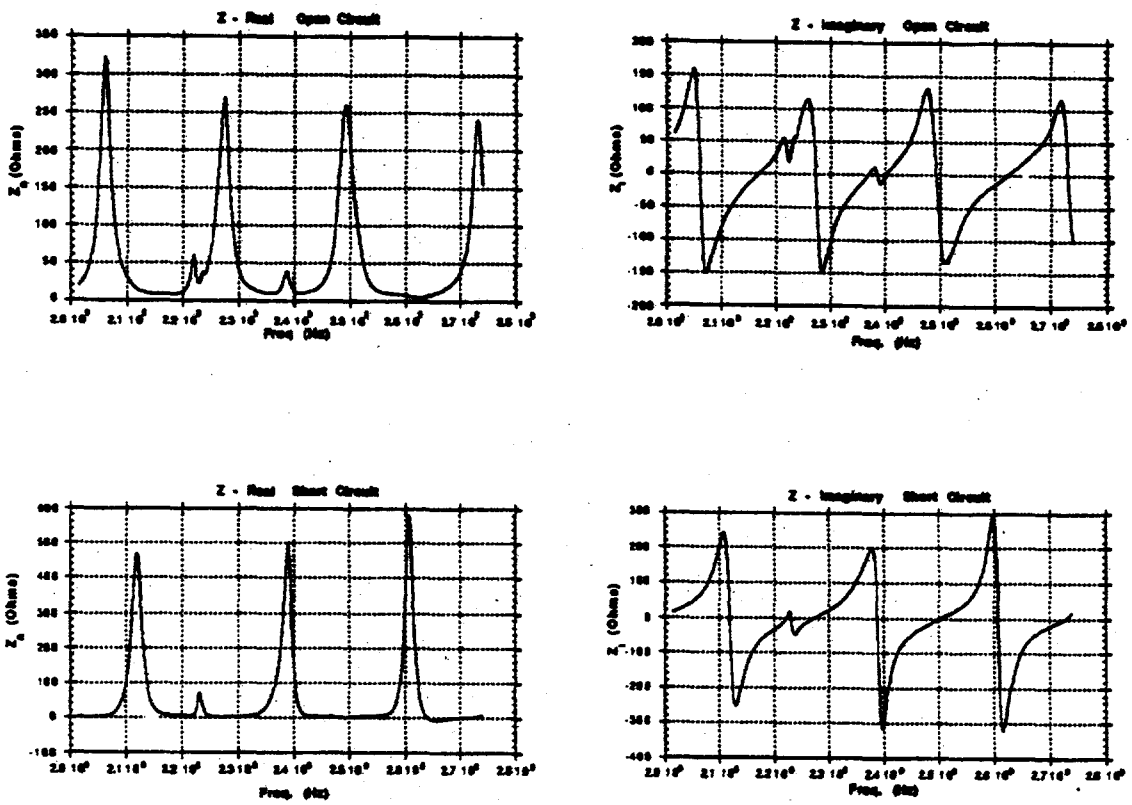

Figure 10. (Upper) Typical real (left) and imaginary(right) components of the stripline impedance with the output port open between 2.20 and 2.74GHz. (Lower) Typical real (left) and imaginary(right) components of the stripline impedance with the output port shorted between 2.20 and 2.74GHz.

The two sets of measurements were then combined to yield the characteristic impedance of the stripline, as shown for the typical measurements in Fig. 11.

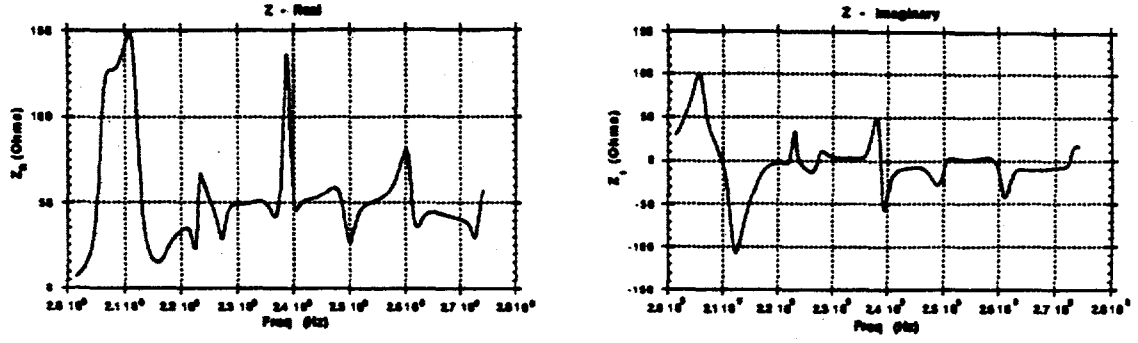

Figure 11. Typical real (left) and imaginary(right) components of the stripline impedance between 2.20 and 2.74GHz.

The frequency regions just above and below 2.5GHz are relatively free of parasitic resonances and are not near the tangent and cotangent poles of the shorted and open impedances, and are therefore target regions for setting resonant frequency. The resonant frequency and coupling are set by adjusting the dimensions in Fig. 12. The length of the center strip determines the resonant frequency as this length is half the guided wavelength

at resonance. With the aluminum oxide dielectric, the 2.5GHz target resonance is achieved with length a little over 2cm. We set the gap width w_1 to yield a minute coupling to the signal source. We then adjusted w_2 to give critical coupling at resonance by starting with a small gap the gradually increasing its width until the network scattering parameter s_{22} vanished. It typically required four iterations to set the gap width. The loaded Q was determined from the transmission width around the resonance, and the unloaded Q was taken to be twice that. Typical room temperature values are:

Quantity	value	uncertainty
Length	2.21cm	0.02cm
w_1	4.60mm	0.05mm
w_2	1.402mm	0.152mm
f_0	2.53366GHz	0.00117GHz
Q_{uni}	362.	17.
Rs	0.072Ω	0.0027Ω

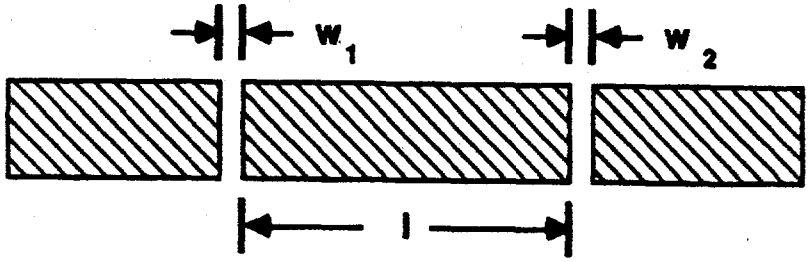

Figure 12. Stripline resonator center strip geometry. The three dimensions are set to give critical coupling at w_2, weak coupling a w_1, and resonant frequency near 2.5GHz.

This procedure quickly determines the microwave surface resistance of materials and results of surface processing. Our large axion experiment uses a right circular cylindrical cavity 0.5m diameter and 1.0m long. Fabricating this cavity is expensive and time consuming and it would not be practical to test materials and processes on the large cavity. This stripline resonator allows for quick evaluation of materials and processing. As an example, Fig. 13 shows a test on a large axion cavity at liquid helium temperature. The vertical axis is Q, the horizontal axis is loading of the output coupler (it is heavily loaded with Q is small, and very weakly coupled when Q is large). Notice that the unloaded Q (in the L band) is over 200k. This is close the theoretical limit set by the anomalous skin depth of copper.

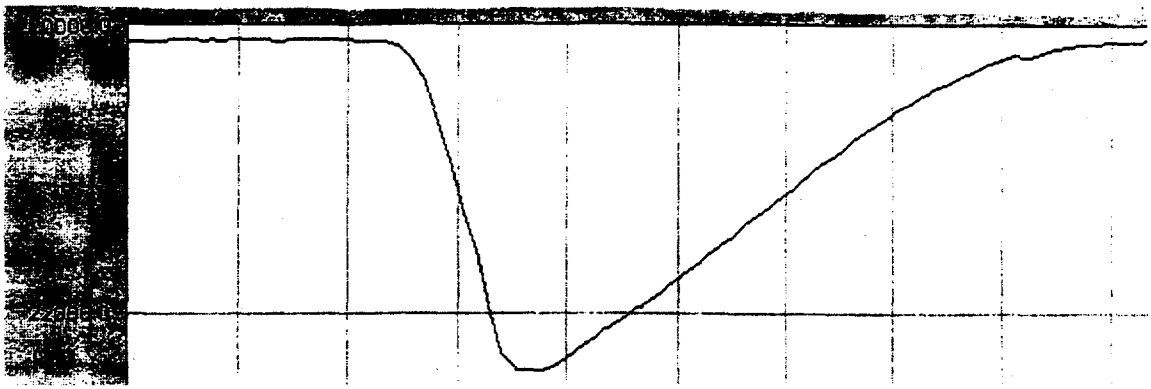

Figure 13. The L-band Q (vertical axis) versus position of the output coupler for the large cavity at liquid helium temperature. The loading is very weak when Q is large, and the loading is strong with Q is small. The unloaded Q is over 200k. This approaches the theoretical limit set by the anomalous skin depth of copper.

4. MEMBERS OF THE MIT AXION GROUP DURING OJI SUPPORT

MIT LNS PPC Group:

L. Rosenberg	(Faculty, Co-spokesman)
H. Peng	(Post doc)
S. Asztalos	(Post doc)
D. Yu	(Grad student)
E. Daw	(Grad student)

5. RECENT AXION GROUP PUBLICATIONS

C.Hagmann et al., Phys. Rev. Lett. **80**, 2043 (1998).
C.Hagmann et al., Rev. Part. Prop. Mini-Review, Euro. Phys. J **C3**, 1 (1998).
L.J.Rosenberg and K.van Bibber, Physics Reports (accepted for publication).
E. Daw, R.Bradley, J. Appl. Phys. **82**, 4 (1997).
M.Mück et al., Appl. Phys. Lett. **72**, 2885 (1998).
H.Peng et al., Nucl. Instrum. Meth. (accepted 1999).
E.Daw et al., Phys. Rev. **D** (to be submitted).